Effects of Cold Rolling on Precipitates in Inconel 718 Alloy

Li Rongbin, Yao Mei, Liu Wenchang, and He Xianchang

(Submitted 9 January 2002; in revised form 8 June 2002)

The morphology, microstructure, and the volume fractions of γ″ phase and δ phase that occur during cold rolling and double aging of Inconel 718 alloy were investigated. Two treatments were developed to produce either single-pass cold rolling or double-pass cold rolling. Cold rolling not only induced the γ″ phase precipitation, but also prompted the γ″→δ phase transformation. Double-pass cold rolling enhanced the δ phase volume fraction, but decreased the γ″ phase volume fraction. The dimension of γ″ particle decreased as cold rolling reduction increased.

Keywords cold rolling, Inconel 718, precipitates

1. Introduction

Inconel 718 Alloy is a nickel-based superalloy largely used in the fabrication of critical components for turbine engines because of its excellent mechanical properties at elevated temperatures and good corrosion resistance. Several works about the precipitation of intermetallic phases in Inconel 718 alloy have been published.[1-6] It has been found that precipitates from the austenite matrix are the metastable γ″ (DO_{22} structure) and γ′ (LI_2 structure) phase and equilibrium δ (DO_a structure) phase.[1-4] The δ phase can form during processing or during service. The precipitation of δ phase during aging has been studied in the solution treated Inconel 718 alloy.[5,7] However, there are only a few studies on the precipitation of δ phase in cold rolling Inconel 718 alloy.[7,8] Singh et al.[8] found that the precipitation of γ″ phase was more prevalent than the precipitation of δ phase for the 30 weight percentage (wt.%) cold-rolled material, and the precipitation of δ phase was more favorable than the precipitation of γ″ phase for the 50 pct cold-rolled material. They thought that the slip bands formed during cold rolling might act as nucleation sites for the δ phase precipitation, which decreases the amount of γ″ phase because there would be insufficient niobium (Nb) present to form the γ″ phase. However, Burke et al.[9] thought that cold working promoted the nucleation of γ″ phase. Obviously, the effect of cold deformation on the precipitation of the γ″ and δ phases cannot be explained clearly. Because the long-term mechanical properties of Inconel 718 alloy are related to the thermal stability, it is important to determine the relationship between cold rolling volume fractions and morphology of γ″ and δ phase in cold rolling Inconel 718 alloy.

However, the influence of different cold rolling practices with different cold rolling reduction on the behavior of the precipitation in Inconel 718 alloying has not been studied. In this work, the aim was to investigate the influence of different cold rolling deformation passes and different cold rolling reduction on the morphology and the volume fraction of γ″ and δ phase.

Li Rongbin and **He Xianchang,** State Key Laboratory of MMCM's, Shanghai Jiaotong University, Shanghai, 200030, China; and **Yao Mei** and **Liu Wenchang,** Institute of Materials Science, Yanshan University, Qinghuangdao, 066004, China. Contact e-mail: rble@sjtu.edu.cn.

2. Experimental Procedure

The Inconel 718 alloy investigated in this article has a composition of 52.4 Ni, 18.87 Cr, 5.26 Nb, 2.95 Mo, 0.98 Ti, 0.54 Al, 0.1 Mn, and 0.041 C, with the Fe comprising the balance (in wt.%). The starting material was received in the form of hot rolling rods with a diameter of 20 mm. These rods were rolled to obtain strips of 10 mm in thickness. These strips were fully solution treated at 970 °C/1 h/air cool, followed by one of two practices: Treatment A, (single-pass cold rolling) strips cold rolled (25, 40, 50, and 65% reduction in thickness, respectively) + direct aged (DA); Treatment B, (double-pass cold rolling) strips cold rolled (25, 40, 50, and 65% reduction in thickness, respectively) + 970 °C/1 h/air cooling + second cold rolling by (25, 40, 50, and 65% reduction in thickness, correspondingly) + DA. The DA heat treatment was used: 720 °C/8 h + furnace cooling at 55 °C/h-620 °C/8 h/air cooling.

Microstructure observation was conducted with transmission electron microscopy (TEM) using an H-800 microscope; the nominal accelerating voltage was 200 kV. The TEM thin films were prepared using the standard method. The samples for x-ray diffraction (XRD) were prepared by mechanical polishing followed by chemical etching on the longitudinal plane. The XRD patterns of Inconel 718 alloy were measured by a D/max-rB x-ray diffractometer at 40 kV and 80 mA with Cu-Kα radiation. The scan rate was 2°/min in the 2θ range from 30-100°. The position of diffraction peaks was calibrated with the use of Si powder. The position-integrated intensities of the diffraction peaks of γ″, δ, and NbC phases were calculated using a software package. The lattice constant of γ phase was calculated with the Nelson-Riley extrapolation method. The wt.% of γ″, γ, and δ phase can be determined by the combination of XRD results and the relationship between the lattice constant of γ phase and the wt.% of γ″, γ′ phases, and δ phase.[10,11] The relationship of the wt.% of γ″, γ′, and δ phases can be described by the following equations:

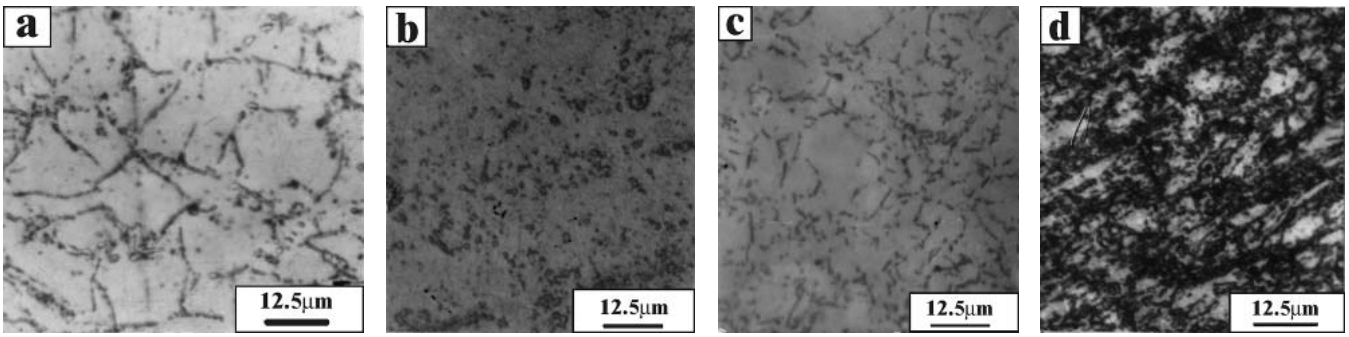

Fig. 1 Effect of cold rolling reduction on microstructure at **(a)** 40% and **(b)** 65% with method A and **(c)** 25% and **(d)** 50% with method B

$$W_\delta = \frac{1 - W\gamma''}{1 + \frac{\rho_{NbC}}{\rho_\delta} \cdot \frac{I_{111}^{NbC}}{\frac{1}{m}\sum_i^m (I_i^\delta / R_i^\delta)} + \frac{\rho_\gamma}{\rho_\delta} \cdot \frac{\frac{1}{n}\sum_i^n (I_i^{\gamma+\gamma'} / R_i^\gamma)}{\frac{1}{m}\sum_i^m (I_i^\delta / R_i^\delta)}} \quad \text{(Eq 1)}$$

$$a = a_0 - \frac{1.9647 \times 10^{-6} W_\delta + 2.4093 \times 10^{-6} W\gamma'' + 0.8435 \times 10^{-6} W_{\gamma'}}{k(k - 0.01526 W_\delta - 0.01508 W_{\gamma''} - 0.01718 W_{\gamma'})} \quad \text{(Eq 2)}$$

$$W_{\gamma'} / W_{\gamma''} = \frac{1}{3} \quad \text{(Eq 3)}$$

where $W_{\gamma''}$ and $W_{\gamma'}$ are the wt.% of γ'' and γ' phases, respectively, a is the lattice constant of γ phase in Inconel 718, $I_i^{\gamma+\gamma'}$ is the combined integrated intensities of the γ and γ' phases, and a_0 is the lattice constant of γ phase when Inconel 718 is solution treated at a temperature of 1040 °C. The value of a_0 depends on the composition of Inconel 718. For the alloy used in this investigation, the value of a_0 is 0.36077 nm. The term k is a constant and can be described by an expression of the form $k = \Sigma(C_i/W_i)$, where C_i is the composition of Inconel 718 in wt.% and W_i is the atomic weight of element i. The calculated value of k is 0.01727 for this alloy. The coefficients in Eq 2 are determined according to the literature.[12] Thus, the wt.% of γ'', γ', and δ phases can be calculated according to the δ, γ, and NbC phases and the lattice constant of γ phase. The error of the wt.% of γ'', γ', and δ phases in this method is mainly related to the accuracy of the measurement of the integrated intensities of the diffraction peaks of δ and γ phases and the accuracy of the measurement of the lattice constant of the γ phase. Their relative errors are within 10%.

3. Results

3.1 Microstructure of Deformation

Figure 1 shows the optical micrographs of the single-pass cool rolling practice (A) and the double-pass cold rolling practice (B) for 25, 40, 50, and 65% reduction cold-rolled samples. Under method A, the grains retain their original equiaxed shapes and the deformation bands in the grain interiors are hardly observed, whereas in increasing the cold rolling reduction to 65%, the grains are elongated and the densities of deformation band in the interior grain increase. Under method B, the sites of precipitate transfer from interior grain to grain boundary, from the slip bands or coplanar flow of dislocation-to-dislocation bands or dislocation walls.

3.2 Morphology of δ Phase

Figure 2 shows the morphology of δ phase under methods A and B with a different reduction in Inconel 718 alloy. It is interesting to note that cold rolling alters the morphology of δ phase. For the 25% cold-rolled sample, the δ phase in the grain interior had needle morphology, and the shape of δ phase changed gradually from needle to spheroid shape with increasing cold rolling reduction.

3.3 Morphology for γ″ Phase

Because reflections of the two types of {100} and {110} positions in [001] orientation could arise both from γ'' and γ' precipitates in Inconel 718 alloy,[13] two distinct morphologies could be observed (Fig. 3): some particles were nearly circular whereas some others were lens shaped. The former corresponded either to the γ' phase or to that γ'' variant for which the tetragonal axis was parallel to the electron beam. The latter corresponded to the other γ'' variant. Those circular precipitates imaged with {100} type as well as {110} type reflections belonged to the γ' phase; those showing up only under {110} type reflections corresponded to the γ'' phase. Some of γ'' particles were ellipsoidal, and many of the γ' particles were a spheroidal shape. Some composite precipitates comprised a hemispherical γ' region with a plate-shaped γ'' region attached to the flat face of the hemisphere. The γ' phase not associated with the γ'' precipitate maintained a spherical shape even when they had grown to large sizes. With increasing cold rolling reduction, the size of γ'' phase dwindled. For example, under method A, the size of γ'' phase was about 13.58 nm (25 wt.%), 13.32 nm (40 wt.%), and 12.2 nm (50 wt.%). It is noted that the second passes cold rolled technology could decrease the size of γ'' phase further, for example, under method B, the size of γ'' phase was 12.62 nm (25 wt.%), 10.74 nm (40 wt.%), and 9.40 nm (50 wt.%).

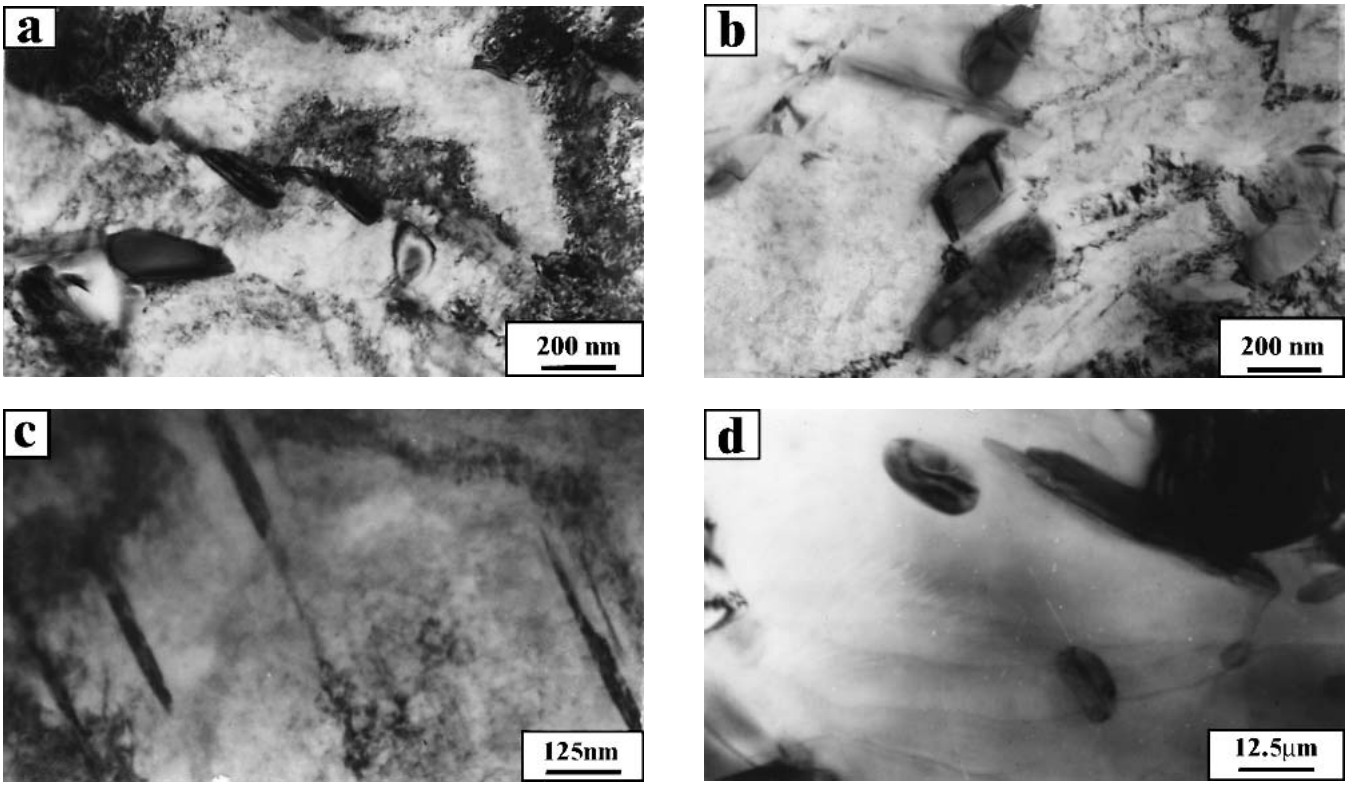

Fig. 2 TEM micrographs showing effects of reduction on δ phase at **(a)** 40% reduction and **(b)** 65% of method A and **(c)** 25% reduction and **(d)** 50% of method B

3.4 Volume Fractions of γ″ and δ Phases

The relationship between the wt.% of γ″ and δ phases and cold rolled reduction is shown in Fig. 4 and 5. The contents of γ″ and δ phases increase as cold-rolled reduction increases under method A. However, for double-pass cold rolling practice (method B), the content of δ phase increased more than that under single-pass cold rolling practice (A) with increasing the cold rolling reduction, and the γ″ phase content varies up and down with increasing cold rolling reduction. Also, the curve shows that the content of γ″ phase varied with increasing reduction; the reasons being the γ″→δ phase transformation and the preferable precipitation of γ″ phase or δ phase.

4. Discussion

4.1 Effects of Cold Rolling on δ Phase

Cold rolling creates not only dislocations, but also excess vacancies. The latter can be attracted to Nb atom segregation[14] to vacancy-absorbing defects such as dislocated cell walls and grain boundaries through the mechanism of non-equilibrium segregation. Because the local Nb supersaturates as the nucleation catalyst is increased, it can be expected that cold rolling affects the thermodynamics of δ phase. Therefore, δ particles can grow into matrix and connect to each other to form needle shapes or laths with little deformation. Thus, the amounts of Nb atom segregation at dislocated cell walls and grain boundaries where δ phase nucleation sites are limits; only δ particles can grow in the shapes of short bar or granular around grain boundaries or dislocated cell walls. As a result, the shape of δ phase changes gradually from needle to short bar or granular as cold rolling reduction increases.

For methods A and B, the δ phase content increased with increasing cold rolling reduction, which suggests that cold rolling promotes precipitation of δ phase. This behavior can be rationalized on the basis of the δ phase nucleation mechanism and the microstructure of cold-rolled Inconel 718 alloy. Because the dislocations are the nucleation sites of δ phase, the dislocations accelerate the diffusion of alloy elements, leading to little diffusion energy in alloy elements. The apparent activation energy of δ precipitation decreases as cold rolling reduction increases, which reveals that cold rolling promotes δ phase precipitation. The curve (Fig. 4) shows that the content of δ phase for the double-pass cold rolling practice (B) is above the amounts for single-pass cold rolling practice (A). The reasons can be attributed to the recrystallization mechanism and deformation mechanism. In fact, at 970 °C, δ phase precipitates in the matrix accompany recovery and recrystallization in cold rolling Inconel 718. The interaction between recrystallization and precipitation has been studied previously in cold rolling Inconel 718 alloy.[15-17] It was found that the austenite recrystallizes and the time of recrystallization finish decreases as cold rolling reduction increases. In addition, the equilibrium concentration of vacancy-Nb atom complexes depends on the concentrations of vacancies and Nb atoms in austenite. At the region of

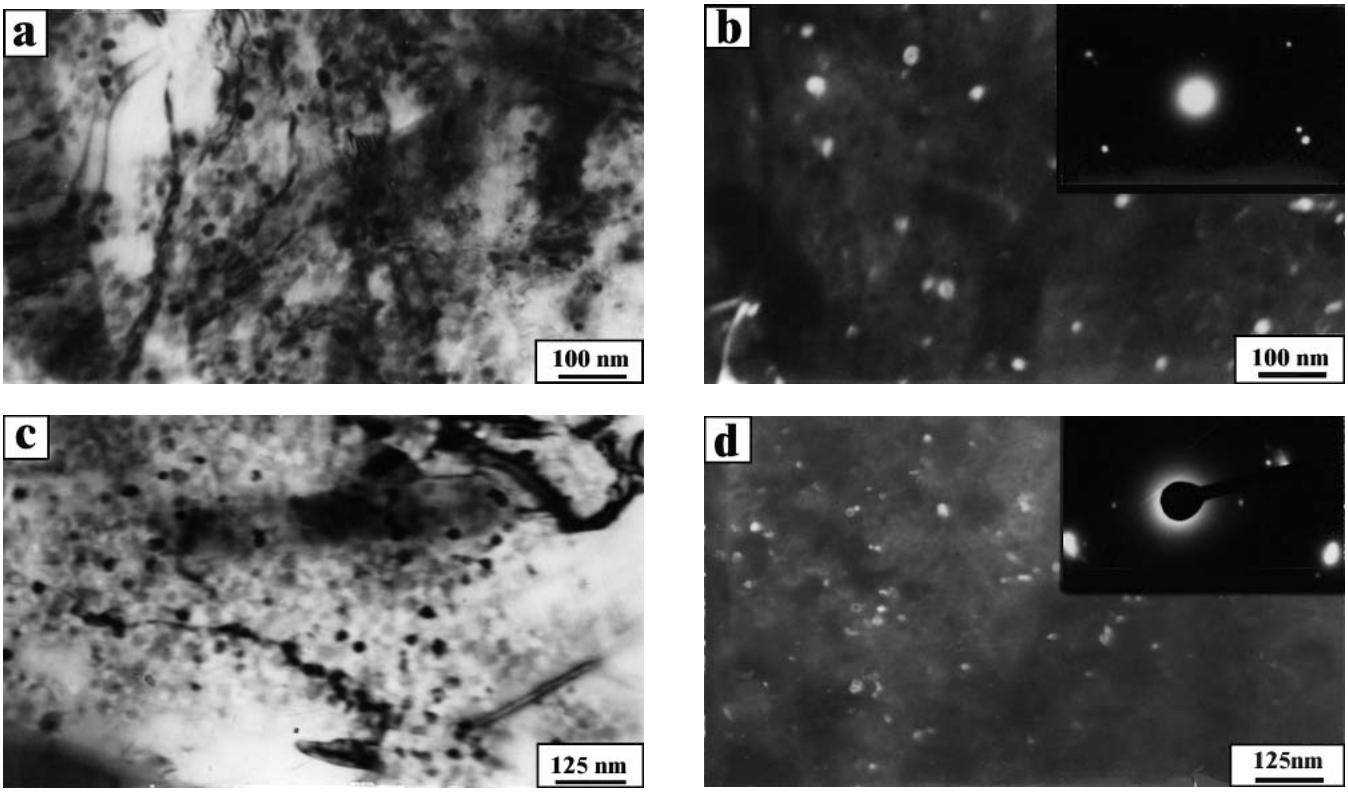

Fig. 3 TEM micrographs showing the microstructure of γ″ and γ′ phases at **(a)** 25% (dark field) and **(b)** 50% of method A and **(c)** 25% (bright field) and **(d)** 65% (dark field) of treatment B. Beam direction is [001]. The insets are the corresponding selected area diffraction patterns.

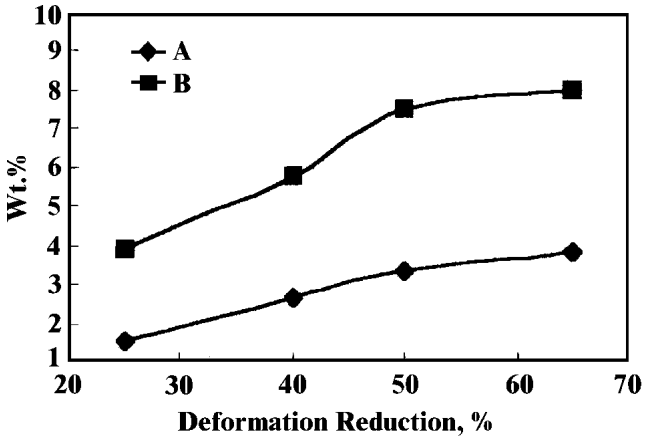

Fig. 4 Effect of deformation reduction on wt.% of δ phase in Inconel 718 for method A and B

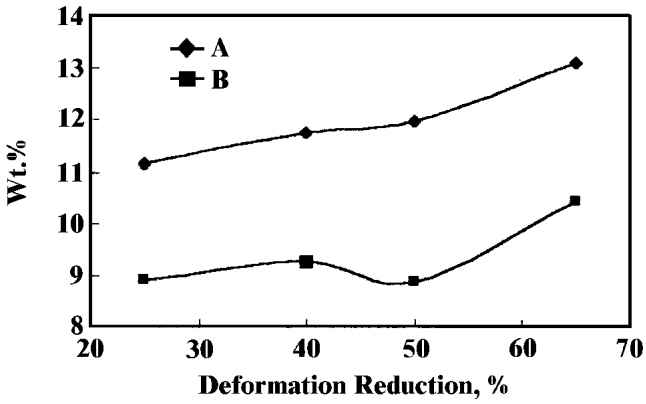

Fig. 5 Effect of deformation reduction on wt.% of γ″ phase in Inconel 718 for method A and B

vacancy-absorbing defects such as dislocated cell walls, the level of excess vacancies is zero, leading to a lower complex concentration there than those in the cell interior. Driven by the concentration gradient, vacancy-Nb atom complexes diffuse toward and are subsequently decomposed at dislocated cell walls, causing Nb atoms to be segregated. The segregation also causes an immediate Nb concentration gradient between dislocated cell walls and the matrix, which leads to a subsequent decrease in integration. However, in comparison with segregation, this is a much slower process because the diffusivity of Nb is significantly slower than that of vacancy-Nb atom complexes.

According to the theory, we can explain the effect of the double-pass cold rolling practice on the precipitation of δ phase. The cold rolling samples solid solution at 970 °C after the single-pass cold rolling deformation has a different time of recovery and recrystallization finish. The time of recrystallization finish for the large cold rolling reduction specimens is shorter than that of the small reduction, and the starting time of δ phase precipitation is much longer than the finish time of recrystallization. As a result, the enrichment of Nb at disloca-

tion cell walls may be retained after the finish of recrystallization. Subsequently, the second cold rolling increases dislocations and causes Nb atoms to be segregated markedly compared with single-passes cold rolling, leading to a prolonged enhancement effect on the precipitation of δ phase.

4.2 Cold Rolling Affects the Precipitation Behavior of γ″ and γ′ Phases

The contents of γ″ and γ′ phases increase as cold rolling reduction increases because of the enhancement effect of cold rolling on the precipitation of γ″ and γ′ phases. Actually, Kirman and Warrington[2] found by TEM that the γ″ phase is sensitive to the excess vacancy concentration of the matrix and that its nucleation is facilitated by the presence of dislocation and extrinsic stacking faults. The enhancement effect of strain on the γ″ precipitation can be attributed to increasing dislocation density, which increases both the nucleation site density and diffusivity of precipitates forming elements in the material. Nb segregation at the grain boundary had been confirmed by Pang et al.[18] in Inconel 718. They found Nb content at the grain boundaries rather than having the grain boundaries acting simply as nucleation sites for preferential precipitation. If Nb segregates at the grain boundaries, Nb can also segregate at dislocations. Nb segregation at dislocations can be expected to facilitate γ″ phase precipitation. Cold rolling promotes not only the precipitation of γ″ phase, but also the γ″→δ phase transformation. The curve in Fig. 5 can be rationalized as follows: The γ″ content first increases and then decreases as cold rolling reduction increases. The increases in γ″ content are due to the enhancement effect of cold rolling on the precipitation of γ″ phase, whereas the decreases in the γ″ content are due to the enhancement effect of cold rolling on γ″→δ phase transformation, and the metastable γ″ particle is replaced by the equilibrium δ particle.[2,5] In addition, strain affects the saturation level of the γ″ precipitation and the incubation time for δ precipitation. As cold rolling reduction increases, the saturation level of the γ″ precipitation increases, whereas the incubation time for δ precipitation decreases. Just after the γ″ content reaches saturation value, the γ″→δ phase transformation occurs. When the precipitation of δ phase was more prevalent than the precipitation of γ″ phase, the content of δ phase increased, and although the δ phase was more favorable than the precipitation of γ″ phase, the γ″ phase content decreased as cold rolling reduction increased. The effect of cold rolling on the γ″→δ phase transformation plays a major role during aging and therefore the γ″ and δ phase varied alternately as cold rolling reduction increase.

5. Conclusions

Cold rolling not only alters the morphology of the deformation microstructure, but also changes the morphology and nucleation site of the δ phase.

Cold rolling promotes not only the precipitation of the δ phase and the γ″ phase but also the γ″→δ transformation. Before the γ″→δ transformation occurs, the γ″ content increased as cold rolling reduction increased, and strain induces the precipitation of γ″ phase. After the γ″→δ transformation occurs, the γ″ content decreases, whereas the δ content increases as cold rolling reduction increases, with strain inducing the γ″→δ transformation.

Double-pass cold rolling increased the δ content compared with single-pass cold rolling practice, but decreased the γ″ content. And the γ″ phase content fluctuated with increasing reduction within 0.8 pct. The dimension of γ″ particles dwindled as cold rolling reduction increased.

Acknowledgment

This work is supported by the National Natural Science Foundation of China under grant No. (59971039).

References

1. D.F. Paulonis, J.M. Oblak, and D.S. Duvall: "Precipitation in Nickel-Base Alloy 718," *Trans. ASM*, 1969, *62*, pp. 611-22.
2. I. Kirman and D.H. Warrington: "The Precipitation of Ni_3Nb Phase in a Ni-Fe-Cr-Nb-Alloy," *Metall. Trans. A.,* 1970, *1*, pp. 2667-75.
3. R. Cozar and A. Pineau: "Morphology of γ″ and γ′ Precipitates and Thermal Stability of Inconel 718 Type Alloy," *Metall. Trans. A,* 1973, *5*, pp. 47-59.
4. J.M. Oblak, D.F. Paulonis, and D.S. Duvall: "Coherency Strengthening in Ni Base Alloys Hardened by DO_{22} γ″ Precipitates," *Metall. Trans. A,* 1974, *5*, pp. 143-53.
5. M. Sundararaman, P. Mukhopadhyay, and S. Banerjee: "Precipitation of δ-Ni_3Nb Phase in Two Nickel Base Superalloys," *Metall. Trans. A,* 1988, *19*A, pp. 453-65.
6. M. Sundararaman, P. Mukhopadhyay, and S. Banerjee: "Some Aspects of the Precipitation of Metastable Intermetallic Phase in Inconel 718," *Metall. Trans. A,* 1992, *23*A, pp. 2015-28.
7. J.L. Burger, R.R. Biederman, and W.H. Couts: "The Effects of Starting Condition on the Aging Response of As-Forged Alloy 718" in *Superalloy 718-Metallurgy and Applications*, E.A. Loria, ed., TMS, Warrendale, PA, 1989 pp. 207-17.
8. R.P. Singh, J.M. Hyzak, T.E. Howson, and R.R. Biederman: "Recrystallization Behavior of Cold Rolled Alloy 718" in *Superalloys 718, 625 and Various Derivatives,* E.A. Loria, ed., TMS, 1991, pp. 205-15.
9. M.G. Burke and M.L. Miller: "Precipitation in Alloy 718: AEM and APFIM Investigation" in *Superalloys 718, 625 and Various Derivatives,* E.A. Loria, ed., TMS, Warrendale, PA, 1991, pp. 337-50.
10. W.C. Liu, F.R. Xiao, M. Yao, and Z.L. Chen: "The Influence of Cold Rolling on the Precipitation of Delta Phase in Inconel 718 Alloy," *Scripta Mater.,* 1997, *37*, pp. 53-57.
11. R.B. Li, M. Yao, W.C. Liu, and X.C. He: Isolation and Determination for δ, γ″ and γ′ Phases in Inconel 718 Alloy," *Scripta Mater.,* 2002, *46*, pp. 635-38.
12. W.C. Liu, F.R. Xiao, M. Yao, and Z.L. Chen: "Relationship Between the Lattice Constant of γ Phase and the Constant of δ Phase, γ″ and γ′ Phases in Inconel 718," *Scripta Mater.,* 1997, *37*, pp. 59-64.
13. M. Sundararaman, P. Mukhopadhyay, and S. Banerjee: "Precipitation and Room Temperature Deformation Behavior of Inconel 718" in *Superalloys 718, 625 and Various Derivatives,* E.A. Loria, ed., TMS, Warrendale, PA, 1994, pp. 419-40.
14. W.C. Liu, M. Yao, and Z.L. Chen: "Niobium Segregation in Inconel 718," *J. Mater. Sci.,* 1999, *34*, pp. 1-4.
15. H. Kreye and E. Hornbogen: "Recrystallisation of Supersaturated Copper-Cobalt Solid Solutions," *J. Mater. Sci.,* 1970, *5*, pp. 89-95.
16. S.S. Hansen, J.B.V. Sande, and M. Cohen: "Niobium Carbonitride Precipitation and Austenite Recrystallization in Hot-Rolled Microalloyed Steels," *Metall. Trans. A,* 1980, *11*A, pp. 387-402.
17. W.C. Liu, M. Yao, and Z.L. Chen: "Recrystallization Behavior of Cold Rolled Inconel 718 Alloy," *J. Aeronautical Mater.,* 1996, *16*(3), pp. 33-38 (in Chinese).
18. X.J. Pang, D.J. Dwyer, and M. Gao: "Surface Enrichment and Grain Boundary Segregation of Niobium in Inconel 718 Single- and Poly-Crystals," *Scripta Mater.,* 1994, *31*, p. 345.